



This discussion paper is/has been under review for the journal The Cryosphere (TC).
Please refer to the corresponding final paper in TC if available.

The stability of grounding lines on retrograde slopes

G. H. Gudmundsson¹, J. Krug², G. Durand^{2,3}, L. Favier², and O. Gagliardini^{2,3}

¹British Antarctic Survey, High Cross, Madingley Rd., Cambridge, CB3 0ET, UK

²Laboratoire de Glaciologie et Géophysique de l'Environnement, UJF-Grenoble, CNRS, Saint-Martin-d'Hères, France

³Institut Universitaire de France, Paris, France

Received: 18 June 2012 – Accepted: 24 June 2012 – Published: 18 July 2012

Correspondence to: G. H. Gudmundsson (ghg@bas.ac.uk)

Published by Copernicus Publications on behalf of the European Geosciences Union.

Stable grounding lines on retrograde slopes

G. H. Gudmundsson
et al.

[Title Page](#)

[Abstract](#)

[Introduction](#)

[Conclusions](#)

[References](#)

[Tables](#)

[Figures](#)

◀

▶

◀

▶

[Back](#)

[Close](#)

[Full Screen / Esc](#)

[Printer-friendly Version](#)

[Interactive Discussion](#)



Abstract

The stability of marine ice sheets grounded on beds that slope upwards in the overall direction of flow is investigated numerically in two horizontal dimensions. We give examples of stable grounding lines on such retrograde slopes illustrating that marine ice sheets are not unconditionally unstable in two-horizontal dimensions. Retrograde bed slopes at the grounding lines of maritime ice sheets, such as the West Antarctic Ice Sheet (WAIS), do not per se imply an instability, nor do they imply that these regions are close to a threshold of instability. We therefore question those estimates of the potential near-future contribution of WAIS to global sea level change based solely on the notion that WAIS, resting on retrograde slope, must be inherently unstable.

1 Introduction

Large parts of the West Antarctica Ice Sheet (WAIS) rest below sea level on a bedrock sloping downwards towards the ice sheet's centre. It has been argued that such marine-type ice sheets on retrograde slopes are inherently unstable and susceptible to rapid disintegration (e.g. Weertman, 1974). The question of WAIS being potentially subject to a marine ice-sheet instability (MISI) is of utmost importance for any quantitative estimates of future sea level change, because it raises the possibility of WAIS rapidly contributing several meters of sea level change.

The possibility of a MISI and the conditions under which such an instability could manifest itself have been investigated by a number of authors. To date most analytical and numerical work has focused on analysing the stability regime of MISI in situations where the problem geometry and the flow field varies primarily in along-flow direction. The problem can then be treated as a problem in one horizontal-dimension (1HD).

In what can be considered to be the first quantitative study of this problem Weertman (1974) concluded that a marine-based ice sheet resting on a retrograde slope is inherently unstable. Further work by Thomas and Bentley (1978) reached similar

TCD

6, 2597–2619, 2012

Stable grounding lines on retrograde slopes

G. H. Gudmundsson
et al.

[Title Page](#)

[Abstract](#)

[Introduction](#)

[Conclusions](#)

[References](#)

[Tables](#)

[Figures](#)

◀

▶

◀

▶

[Back](#)

[Close](#)

[Full Screen / Esc](#)

[Printer-friendly Version](#)

[Interactive Discussion](#)



Stable grounding lines on retrograde slopes

G. H. Gudmundsson
et al.

[Title Page](#)

[Abstract](#) [Introduction](#)

[Conclusions](#) [References](#)

[Tables](#) [Figures](#)

◀

▶

◀

▶

[Back](#)

[Close](#)

[Full Screen / Esc](#)

[Printer-friendly Version](#)

[Interactive Discussion](#)



Stable grounding lines on retrograde slopes

G. H. Gudmundsson
et al.

[Title Page](#)

[Abstract](#)

[Introduction](#)

[Conclusions](#)

[References](#)

[Tables](#)

[Figures](#)

◀

▶

◀

▶

[Back](#)

[Close](#)

[Full Screen / Esc](#)

[Printer-friendly Version](#)

[Interactive Discussion](#)



model where the degree of ice-shelf buttressing at the grounding line was in effect prescribed through a side-drag parametrisation. It is unclear what three-dimensional geometrical configuration, if any, gives rise to the type of prescribed side drag used by Dupont and Alley (2005) in their example. Goldberg et al. (2009) performed a series 5 of numerical experiments using a vertically integrated model that accounted for all the stress terms in 2HD otherwise missing in vertically integrated 1HD models. One of their numerical experiments suggested that ice-shelf buttressing might restore stability and they concluded that a further investigation was warranted.

The strongest recent claim in this regard was given by Katz and Worster (2010). 10 They investigated the stability of ice-sheet grounding lines in 2HD numerically using a vertically integrated formulation of the force balance at the grounding line, and concluded that unstable retreat of grounding lines over retrograde beds is a “robust” feature of such models. Katz and Worster (2010) assumed the stress vector at the grounding line to be aligned in the direction normal to the grounding line. Their model study did 15 therefore not fully account for the variation of stresses in 2HD. The fact that Katz and Worster (2010) did not find an example of a stable grounding line on a retrograde slope in 2HD clearly does not exclude the possibility that such an example may exist.

It is, hence, currently not clear if the MISI applies unconditionally in 2HD. On the other hand, to date neither an analytical or a numerical example of a stable grounding- 20 line configuration of a maritime ice sheet resting on a retrograde slope has been found. The purpose of this work is to provide such an example, and to show that the MISI does not hold unconditionally in 2HD.

2 Problem definition

The model setup is motivated by the “Marine Ice Sheet Model Intercomparison Project” 25 (MISMIP) experiment 3 (Pattyn et al., 2012), and can be considered to represent a three-dimensional (i.e. two horizontal dimensional) extension of that problem. The MISMIP experiment 3 was in turn inspired by Schoof (2007a) who, in his analysis of

grounding-line dynamics in one-horizontal dimension, used a particular type of bed profile to demonstrate the marine instability mechanism. This MISMIP experiment 3 has become a benchmark case for assessing and testing the capability of numerical models to simulate the advance and retreat of the grounding line. The experiment also provides a striking example of the marine instability mechanism in 1HD.

The model domain used here stretches from 0 to 1800 km in x direction, and from -120 to 120 km in y direction. For $x = 0$, both horizontal velocity components are set to zero, i.e. $u(0, y) = v(0, y) = 0$, and along the sides where $y = \pm 120$ km, the y component is set to zero, i.e. $v(x, \pm 120\text{ km}) = 0$.

The bed geometry used here can be written as

$$B(x, y) = B_x(x) + B_y(y), \quad (1)$$

where

$$\begin{aligned} B_x(x) = & B_0 - 2184.8 (x/750 \times 10^3)^2 \\ & + 1031.72 (x/750 \times 10^3)^4 \\ & - 151.72 (x/750 \times 10^3)^6, \end{aligned} \quad (2)$$

and

$$B_y(y) = \frac{d_c}{1 + e^{-2(y - w_c)/f_c}} + \frac{d_c}{1 + e^{2(y + w_c)/f_c}}, \quad (3)$$

where the units are meters, and $B(x, y)$ stands for the topography of the ocean floor.

The bed is in the form of a channel incised into a slowly undulating plane with an overall downward slope in x direction (see Fig. 1). The parameter f_c controls the slope of the flanks, d_c controls the depth of the channel, and w_c is the half-width of the channel. The only parameter that is varied in the model runs described below is the half-width (w_c).

Stable grounding lines on retrograde slopes

G. H. Gudmundsson
et al.

[Title Page](#)

[Abstract](#)

[Introduction](#)

[Conclusions](#)

[References](#)

[Tables](#)

[Figures](#)

◀

▶

◀

▶

[Back](#)

[Close](#)

[Full Screen / Esc](#)

[Printer-friendly Version](#)

[Interactive Discussion](#)



[Title Page](#)[Abstract](#)[Introduction](#)[Conclusions](#)[References](#)[Tables](#)[Figures](#)[◀](#)[▶](#)[◀](#)[▶](#)[Back](#)[Close](#)[Full Screen / Esc](#)[Printer-friendly Version](#)[Interactive Discussion](#)

As can be seen from Eqs. (1)–(3), the slope of the bed in x direction is independent of y , i.e. $\partial_{yx}^2 B(x, y) = 0$. The slope in x direction is zero at $x = 0$, $x = x_a$ and $x = x_b$ where $x_a = 973.7$ km and $x_b = 1265.7$ km, and for $x_a < x < x_b$ the bed slopes upwards ($\partial_x B(x, y) > 0$) and is retrograde across the entire domain, i.e. $\partial_x B(x, y) > 0$ for $x_a < x < x_b$ independently of y . The values for the geometrical parameters B_0 , f_c , d_c used in all runs are listed in Table 1.

3 Numerical models

We use two different numerical models: a full Stokes model, and a vertically integrated model of a type commonly used in glaciology to model the flow of ice sheets and ice streams. Both models are based on the finite elements method and both are capable of using unstructured grids with spatially variable element sizes. The full Stokes solver uses the open source finite element software package Elmer and the solver will be referred to here as “*Elmer/Ice*”. The equations representing the vertically integrated model are solved using a finite element code developed by one of the authors (G. Hilmar Gudmundsson), and the code will here be referred to as “*Úa*”. Most of the calculations presented here were obtained with *Úa*. The *Elmer/Ice* code was primarily used to demonstrate that the some key aspects of the results obtained with *Úa* are not specific to that model.

The full Stokes model includes all the terms of the Stokes equations, i.e.

$$20 \quad \sigma_{pq,q} + f_p = 0, \quad (4)$$

where σ_{pq} are the components of the Cauchy stress tensor, and f_p the components of the body force, with $f = \rho g(0, 0, -1)^T$.

The vertically integrated model solves a simplified stress balance that can be written on the form

$$25 \quad \nabla_h^T \cdot (h \sigma_h) + t_{bh} = \rho g h \nabla_h s, \quad (5)$$

where

$$\sigma_h = \begin{pmatrix} 2\tau_{xx} + \tau_{yy} & \tau_{xy} \\ \tau_{xy} & 2\tau_{yy} + \tau_{xx} \end{pmatrix}, \quad (6)$$

with

$$\nabla_h^T = (\partial_x, \partial_y), \quad (7)$$

5 where h , when used as a subscript, is a mnemonic for “horizontal”. In the above equation τ_{ij} are the components of the deviatoric stress tensor, s is the surface topography, h is the ice thickness, ρ is the ice density, g is the gravitational acceleration, and t_{bh} is the horizontal part of the bed-tangential basal traction t_b where

$$t_b = \sigma \hat{n} - (\hat{n}^T \cdot \sigma \hat{n}) \hat{n}, \quad (8)$$

10 with \hat{n} being a unit normal vector to the bed pointing into the ice.

Both models employ the Weertman sliding law

$$t_b = C^{-1/m} |\mathbf{v}_b|^{1/m-1} \mathbf{v}_b, \quad (9)$$

where \mathbf{v}_b

$$\mathbf{v}_b = \mathbf{v} - (\hat{n}^T \cdot \mathbf{v}) \hat{n}, \quad (10)$$

15 is the basal sliding velocity, C is the basal slipperiness, and m a stress exponent.

Both models also employ Glen's flow law

$$\dot{\epsilon}_{ij} = A \tau^{n-1} \tau_{ij}, \quad (11)$$

where τ is the second invariant of the deviatoric stress tensor

$$\tau = \sqrt{\tau_{pq} \tau_{pq} / 2}, \quad (12)$$

Stable grounding lines on retrograde slopes

G. H. Gudmundsson
et al.

[Title Page](#)

[Abstract](#)

[Introduction](#)

[Conclusions](#)

[References](#)

[Tables](#)

[Figures](#)

◀

▶

◀

▶

[Back](#)

[Close](#)

[Full Screen / Esc](#)

[Printer-friendly Version](#)

[Interactive Discussion](#)



$\dot{\epsilon}_{ij}$ are the strain rates, A is the rate factor, and n a stress exponent.

In addition to the equations above (and not listed here) both models use appropriate forms of the mass-conservation equation for an incompressible medium, and employ the kinematic boundary conditions along free upper and lower surfaces.

5 Along the calving front a pressure boundary condition is applied that corresponds to ocean surface level at $z = 0$, i.e.

$$\sigma \hat{n} = -\rho_w \hat{n}, \quad (13)$$

where $\hat{\mathbf{n}}$ is a unit normal vector pointing horizontally outward from the ice front, and p_w is the hydrostatic pressure in the ocean. The surface of the ocean (S) is at $S = 0$, and the oceanic pressure is $p_w = \rho_w g(S - z)$ for $z < S$ and zero otherwise, where ρ_w is the ocean density.

For vertically integrated models the boundary condition at the ice-shelf edge at $x = 1800\text{ km}$ takes the form

$$\sigma_h \hat{n} = \frac{1}{2} \rho g h \hat{n}, \quad (14)$$

15 provided the ice is fully floating at the calving front, and where

$$\rho = \rho(1 - \rho/\rho_w) \quad (15)$$

In the vertically integrated model the floating condition takes the form $h < h_f$ where

$$h_f = \rho_w H / \rho, \quad (16)$$

20 where H is the ocean depth. The quantity h_f represents the maximum possible ice-shelf thickness at any location. A detailed description of the contact condition that arises in the treatment of the grounding-line in the full Stokes model, and its implementation, is given in Favier et al. (2012).

The vertically integrated model used here is one of the most commonly used models in glaciology for describing the flow of ice shelves and ice streams. Derivation of the

model can be found, for example, in Hutter (1983), Morland (1984), Muszynski and Birchfield (1987), MacAyeal (1989), and Baral and Hutter (2001) and properties of the linearised equations are discussed in some detail in Gudmundsson (2008).

The two numerical codes, i.e. *Elmer/Ice* and *Ua*, have been used extensively in the past to calculate grounding-line migrations for various different setups (Durand et al., 2009a; Gagliardini et al., 2010; Pattyn et al., 2012). Both models participated in the recently finalised “Marine Ice Sheet Model Intercomparison Project” (MISMIP) (see Pattyn et al., 2012) and results from these two models were submitted to the ongoing “Marine Ice Sheet Model Intercomparison Project for Planview Models” (MISMIP3D).

Automated remeshing was used to ensure a highly dense discretisation of the area around the grounding line. Calculations of grounding-line migration are known to require a finely resolved mesh around the grounding-line area (e.g. Durand et al., 2009b). How accurate the mesh needs to be is a question that is difficult to answer a priori, but can be answered easily by performing a number of runs using increasingly fine meshes until no resolution dependent behaviour is seen.

Runs performed with solver *Ua* were done using linear, quadratic, and cubic triangular elements, however the set of results from *Ua* shown here were obtained using quadratic elements. The *Elmer/Ice* solver used linear prismatic elements stabilised using the bubble-stabilising method. The exact sizes and number of elements varied between runs, but, as an example, results shown below using *Ua* for a half-width of $w_c = 50$ km used a mesh of 228 537 elements with 457 340 nodes, with median, maximum and minimum element sizes of 569 m, 26 862 m, and 86.7 m, respectively.

A fully implicit forward integration procedure was used by *Ua*, with the prognostic and the diagnostic equations being solved simultaneously using the Newton-Raphson method. Further details of the solution procedure of the full Stokes model *ELMER/Ice* can be found in Durand et al. (2009a).

Stable grounding lines on retrograde slopes

G. H. Gudmundsson et al.

[Title Page](#)

[Abstract](#)

[Introduction](#)

[Conclusions](#)

[References](#)

[Tables](#)

[Figures](#)

◀

▶

◀

▶

[Back](#)

[Close](#)

[Full Screen / Esc](#)

[Printer-friendly Version](#)

[Interactive Discussion](#)



4 Results

A number of runs using the parameters listed in Table 1 and the bed geometry defined by Eqs. (1)–(3) were performed and the runs continued until steady state was reached. Steady state was considered to have been reached once both the mean rate of surface elevation change over the surface nodes was less than 0.001 m a^{-1} .

The values used for surface accumulation a , the slipperiness parameter C and the stress exponent m in Weertman's sliding law (Eq. 9), and the stress exponent n in Glen's flow law (Eq. 11) are identical to those used in MISMIP experiment 3a (see Pattyn et al., 2012). The surface accumulation, a , is set at $a = 0.3\text{ m a}^{-1}$ across the whole surface. Note that the surface accumulation is in units of ice equivalent, and the actual mass flux across the surface is $\rho a = 270\text{ kg a}^{-1}\text{ m}^{-2}$.

An example of calculated steady-state grounding-line position is given in Fig. 2. This particular run was obtained with $\dot{U}a$ for $w_c = 50\text{ km}$. Note that in Fig. 2 only a part of the model domain is shown and that the whole domain stretches in x direction from 0 to 1800 km. A perspective plot of the same model output, showing the whole model domain, is given in Fig. 3.

As Fig. 2 shows the grounding line (shown in black) curves considerably within the xy plane. At the left and right-hand side margins of the numerical domain ($y = \pm 120\text{ km}$), the grounding line is located at approximately $x = 1400\text{ km}$. Where the grounding line crosses the medial line ($y = 0$), it is located at about $x = 1100\text{ km}$. As a consequence, a sizable confined ice shelf is formed. The upper and lower limits of retrograde bed slope, $x_a = 973.7\text{ km}$ and $x_b = 1265.7\text{ km}$, are marked by two cyan lines in the Fig. 2. As the figure illustrates, sections of stable grounding line are located on retrograde slopes.

The position of the grounding line with respect to the bed is shown in Fig. 3. Inspection of Figs. 2 and 3 reveals that the highest velocities along the grounding line, and the largest ice thicknesses, are found in the area of retrograde slope.

TCD

6, 2597–2619, 2012

Stable grounding lines on retrograde slopes

G. H. Gudmundsson et al.

[Title Page](#)

[Abstract](#)

[Introduction](#)

[Conclusions](#)

[References](#)

[Tables](#)

[Figures](#)

◀

▶

◀

▶

[Back](#)

[Close](#)

[Full Screen / Esc](#)

[Printer-friendly Version](#)

[Interactive Discussion](#)



Stable grounding lines on retrograde slopes

G. H. Gudmundsson
et al.

[Title Page](#)

[Abstract](#)

[Introduction](#)

[Conclusions](#)

[References](#)

[Tables](#)

[Figures](#)

◀

▶

◀

▶

[Back](#)

[Close](#)

[Full Screen / Esc](#)

[Printer-friendly Version](#)

[Interactive Discussion](#)



The steady-state geometries shown in Figs. 2 and 3 were arrived at by starting with an initial constant ice thickness of 100 m. The solution converged slowly to the steady-state solution shown in the figures in span of several thousand of years, and the possibility of the steady-state being unstable can be excluded. The results obtained with *Elmer/Ice* were arrived at by starting with the final geometry as given by *Úa* and run until a new steady-state was reached.

Comparison between results obtained by *Elmer/Ice* and *Úa* is given in Fig. 4. As can be seen the surface profiles obtained with the two models closely agree, and in both cases the grounding line is located at a section of the bed with a retrograde slope.

Runs were performed with half-widths (w_c) ranging from 20 to 70 km, as well as for the limiting cases of $w_c = 0$ and $w_c = \infty$. Each run was started by taking a model geometry from a previous run for a similarly shaped bedrock as a starting point. Again the possibility of the models runs converging with time to an unstable steady-state can be excluded.

The steady-state grounding-line position (x_{gl}) at the medial line ($y = 0$) for several different models with half-widths (w_c) ranging from 20 to 70 km is shown in Fig. 5. These calculations were performed for the vertically integrated model (see Eq. 5) with the numerical code *Úa*. The results indicate a gradual change in grounding-line position as a function of channel width. Several cases of stable steady-state grounding lines located on retrograde slopes were found. As expected, the grounding line is no longer located on retrograde slopes for both large and small w_c values. Figure 5 suggest that, for this particular parameter set used (see Table 1), grounding lines are located on retrograde slopes for w_c within the approximate of 35 to 55 km.

A close inspection of Fig. 2 reveals that at around $(x, y) = (1400, \pm 50)$ km, the grounding line (shown in black) extends some distance downstream and appears to break up in a few isolated regions of grounded ice. This is not an artefact of the figure. In this area the ice is either grounded or close to be grounded, and in the course of the transient run towards steady state various smaller patches of ice become either grounded or ungrounded.

Stable grounding lines on retrograde slopes

G. H. Gudmundsson
et al.

[Title Page](#)

[Abstract](#)

[Introduction](#)

[Conclusions](#)

[References](#)

[Tables](#)

[Figures](#)

◀

▶

◀

▶

[Back](#)

[Close](#)

[Full Screen / Esc](#)

[Printer-friendly Version](#)

[Interactive Discussion](#)



A further, in our view an entirely realistic, feature found in a number of our model runs are small (on the order of one ice thickness in horizontal dimension) regions of thin ice that form downstream of the grounding line within the unconfined section of the ice-shelf. For numerical purposes, the thickness was forced to be slightly positive. In the runs shown here, the minimum thickness was set at 10 m. This thickness constraint was implemented in a similar manner in both *Elmer/Ice* and *Ua*. The method used in *Elmer/Ice* is described in Durand et al. (2009a). The *Ua* solver uses for this purpose an active-set method where any violated thickness constraints are activated using Lagrange multiplier approach. The modified system is then solved again, and the sign of the Lagrange multipliers (or “slack variables” as these variables are sometimes referred to in this context) used to determine if an active constraint should subsequently be inactivated, or if further constraints need to be included in the active set. This procedure is repeated until the active set no longer changes, before progressing to next time step. The number of active constraints differed between runs and changed in the course of the transient calculations, but the number of active nodal constraints was usually less than 10. For the final steady-state solution shown in Fig. 2, for example, the thickness constraint was activated at 7 nodes in total (the total number of nodes in the finite-element mesh at the end of this run was 457 340). These 7 nodes were located at approximately $(x, y) = (1460, \pm 88)$ km. This is a region of the ice-shelf that is subjected to strong longitudinal extension and comparatively small concomitant transverse compression. Runs with different minimum ice thickness constraints of 1 m, and 0.1 m, showed that the exact value of the thickness constraint used was, for the purpose of the model exercise, irrelevant, and had no effect of whether the grounding line was located on a retrograde slope or not.

25 5 Discussion

The basis for the MISI is the idea of ice flux at the grounding line being a monotonically increasing function of ice thickness (h_{gl}) at the grounding line. If this holds, then

a simple heuristic argument (Weertman, 1974) shows steady-state grounding-line positions of marine-type ice sheets on retrograde slopes to be unstable. As shown by Schoof (2007b) ice flux can be expressed as a function of both h_{gl} and longitudinal stress, with ice flux being an increasing function of both of these variables. It turns out that in 1HD, longitudinal stress is also an increasing function of thickness and, hence, ice flux always an increasing function of h_{gl} in 1HD. It is important to realise that this argument does not hold in 2HD. In 2HD it is conceivable, in principle, to have a configuration where longitudinal stress decreases with thickness with the overall effect of flux being a decreasing function of thickness. In that case, the MISI is not expected to operate and a stable grounding-line positions on a retrograde slopes become a possibility. However, hitherto, no such example of a stable grounding line in 2HD has been provided.

The absence of such a specific counter-example may have been taken to suggest that the MISI applies unconditionally to the 2HD situation. Observations of grounding lines located on reverse bed slopes have been used repeatedly in the past as the sole basis on which to argue that large sections of WAIS are either unstable, or close to a threshold of instability (e.g. Ross et al., 2012). Some recent estimates (e.g. Bamber et al., 2009) of potential sea-level rise from WAIS implicitly assume that MISI operates in 2HD. By providing a numerical example of a marine-type ice sheet in a stable steady-state configuration with the grounding line located on a retrograde slope we have now shown marine ice sheets to be conditionally stable. Our finding that marine-type ice sheets on retrograde slopes are not unconditionally stable do not contradict, and are fully compatible with, theoretical and numerical work showing that, in one horizontal dimension, rapidly sliding marine ice sheets on retrograde slopes are unconditionally unstable.

For our particular parameter set (see Table 1) we find stable grounding-line positions for half-widths between the approximate range of 35 to 55 km. We do not expect this range of half-widths values (w_c) to remain the same for other parameter sets. Neither do we expect the existence of stable grounding-line positions on retrograde slopes to

Stable grounding lines on retrograde slopes

G. H. Gudmundsson
et al.

[Title Page](#)

[Abstract](#)

[Introduction](#)

[Conclusions](#)

[References](#)

[Tables](#)

[Figures](#)

◀

▶

◀

▶

[Back](#)

[Close](#)

[Full Screen / Esc](#)

[Printer-friendly Version](#)

[Interactive Discussion](#)

Stable grounding lines on retrograde slopes

G. H. Gudmundsson
et al.

[Title Page](#)

[Abstract](#)

[Introduction](#)

[Conclusions](#)

[References](#)

[Tables](#)

[Figures](#)

[◀](#)

[▶](#)

[◀](#)

[▶](#)

[Back](#)

[Close](#)

[Full Screen / Esc](#)

[Printer-friendly Version](#)

[Interactive Discussion](#)



be a simple function of channel widths. The stability regime can be expected to be primarily determined by the level of ice-shelf buttressing at the grounding line, with the buttressing in turn being a (potentially complicated) function of bed geometry and ice rheology. The stability of a given marine ice-sheet configuration can most likely not be assessed from geometrical considerations (bedrock slope, ice-stream width, etc.) only, and each situation may require targeted modelling efforts.

In many situations the *sensitivity* of ice sheets to external forcing is of key interest. We stress that here we have only addressed the very different question of the *stability* of marine-type ice sheets. Our results do not, for example, exclude the possibility that the sensitivity of the grounding-line position to changes in basal melt rates depends on bed slopes. Note in this respect that in 1HD (and provided the horizontal variation of shear stresses can be ignored), the grounding-line position is independent of any forcing to which the ice shelf is subjected to. In other words, in 1HD the sensitivity of (stable) grounding-line positions to oceanic forcing is not only independent of bed slope, but zero. Although we have not investigated this possibility here, we find it likely that the 2HD situation is, in this respect, also sharply different from the 1HD case. Numerical modelling has shown ice sheets to respond to changes in ice-shelf melting in complicated and at times non-intuitive ways (Gagliardini et al., 2010). We consider it likely that the sensitivity of ice-sheets to ocean forcing is dependent on bed geometry and bed slope, and we do not discard the possibility that ice sheets may be highly sensitive in this respect for some particular bed geometries.

6 Conclusions

We have provided specific numerical examples of model geometries for which sections of stable grounding lines are located on retrograde slopes. We conclude that maritime ice sheets on retrograde slopes are not unconditionally unstable.

Our confidence in our model results is strengthened by the fact that we have solved the flow problem using two different numerical codes (*Ua* and *Elmer/Ice*), based on two different set of model assumptions.

The conditional stability in 2HD does not contradict previous findings of unconditional instability in 1HD. These differences simply show that the 1HD and the 2HD problems differ fundamentally in this respect. Real ice sheets are of course three dimensional features and we caution against applying arguments to ice sheets that are inherently tied to 1HD. These stark differences between the 1HD and the 2HD cases should also be considered in any applications of 1HD flow-line models, and the use of 1HD flow-line models to investigate the stability regime of marine ice sheets is problematic.

Observations of retrograde bed slopes at the grounding lines of maritime ice sheets, such as the West Antarctic Ice Sheet, do not as such imply an unstable mode of retreat or advance, nor do they imply that such regions are close a threshold of instability. Questions regarding stability of a given marine ice-sheet configuration are unlikely to be answered without targeted modelling efforts.

Acknowledgements. This work was supported by NERC grant Nr. NE/H02333X/1. The *Elmer/Ice* simulations were granted access to the HPC resources of Lindgren (PDC, Sweden) made available within the “Distributed European Computing Initiative” by the PRACE-2IP, funded in part by the European Community’s Seventh Framework Programme (FP7/2007-2013) under grant agreement Nr. RI-283493.

The support by J. Vosper, constructive comments from D. G. Vaughan, and extended and very usu full discussions with R. Arthern are acknowledged.

References

Bamber, J. L., Riva, R. E. M., Vermeersen, B. L. A., and LeBrocq, A. M.: Reassessment of the potential sea-level rise from a collapse of the West Antarctic ice sheet, *Science*, 324, 901–903, doi:10.1126/science.1169335, available at: <http://www.sciencemag.org/content/324/5929/901.abstract>, 2009. 2609

TCD

6, 2597–2619, 2012

Stable grounding lines on retrograde slopes

G. H. Gudmundsson
et al.

[Title Page](#)

[Abstract](#)

[Introduction](#)

[Conclusions](#)

[References](#)

[Tables](#)

[Figures](#)

◀

▶

◀

▶

[Back](#)

[Close](#)

[Full Screen / Esc](#)

[Printer-friendly Version](#)

[Interactive Discussion](#)



Baral, D. R. and Hutter, C.: Asymptotic theories of ice sheets and ice shelves, in: *Geomorphological Fluid Mechanics*, edited by: Balmforth, N. J. and Provenzale, A., *Lecture Notes in Physics*, chap. 11, 227–278, Springer, Heidelberg, 2001. 2605

Dupont, T. K. and Alley, R. B.: Assessment of the importance of ice-shelf buttressing to ice-sheet flow, *Geophys. Res. Lett.*, 32, L04503, doi:10.1029/2004GL022024, 2005. 2599, 2600

Durand, G., Gagliardini, O., de Fleurian, D., Zwinger, T., and Meur, E. L.: Marine ice sheet dynamics: hysteresis and neutral equilibrium, *J. Geophys. Res.*, 114, F03009, doi:10.1029/2008JF001170, 2009a. 2605, 2608

Durand, G., Gagliardini, O., Zwinger, T., Meur, E. L., and Hindmarsh, R.: Full-Stokes modeling of marine ice-sheets: influence of the grid size, *Ann. Glaciol.*, 50, 109–114, 2009b. 2605

Favier, L., Gagliardini, O., Durand, G., and Zwinger, T.: A three-dimensional full Stokes model of the grounding line dynamics: effect of a pinning point beneath the ice shelf, *The Cryosphere*, 6, 101–112, doi:10.5194/tc-6-101-2012, 2012. 2604

Gagliardini, O., Durand, G., Zwinger, T., Hindmarsh, R. C. A., and Meur, E. L.: Coupling of ice-shelf melting and buttressing is a key process in ice-sheets dynamics, *Geophys. Res. Lett.*, 37, doi:10.1029/2010GL043334, 2010. 2605, 2610

Goldberg, D., Holland, D. M., and Schoof, C.: Grounding line movement and ice shelf buttressing in marine ice sheets, *J. Geophys. Res.*, 114, F04026, doi:10.1029/2008JF001227, 2009. 2600

Gudmundsson, G. H.: Analytical solutions for the surface response to small amplitude perturbations in boundary data in the shallow-ice-stream approximation, *The Cryosphere*, 2, 77–93, doi:10.5194/tc-2-77-2008, 2008. 2605

Hindmarsh, R. C. A.: Qualitative dynamics of marine ice sheets, in: *Ice in the Climate System*, edited by: Peltier, W. R., no. 12 in *NATO ASI Series I*, 66–99, Springer, Dordrecht, Holland, 1993. 2599

Hindmarsh, R. C. A.: Stability of ice rises and uncoupled marine ice sheets, *Ann. Glaciol.*, 23, 94–104, 1996. 2599

Hutter, K.: *Theoretical Glaciology; Material Science of Ice and the Mechanics of Glaciers and Ice Sheets*, D. Reidel Publishing Company/Tokyo, Terra Scientific Publishing Company, 1983. 2605

Katz, R. F. and Worster, M. G.: Stability of ice-sheet grounding lines, *P. Roy. Soc. A.Math., Phys.*, 466, 1597–1620, doi:10.1098/rspa.2009.0434, 2010. 2600

TCD

6, 2597–2619, 2012

Stable grounding lines on retrograde slopes

G. H. Gudmundsson
et al.

[Title Page](#)

[Abstract](#)

[Introduction](#)

[Conclusions](#)

[References](#)

[Tables](#)

[Figures](#)

◀

▶

◀

▶

[Back](#)

[Close](#)

[Full Screen / Esc](#)

[Printer-friendly Version](#)

[Interactive Discussion](#)



MacAyeal, D. R.: Large-scale ice flow over a viscous basal sediment: theory and application to ice stream B, Antarctica, *J. Geophys. Res.*, 94, 4071–4078, 1989. 2605

Morland, L. W.: Thermomechanical balances of ice-sheet flows, *Geophys. Astro. Fluid*, 29, 237–266, 1984. 2605

Muszynski, I. and Birchfield, G. E.: A coupled marine ice-stream-ice – shelf model, *J. Glaciol.*, 33, 3–14, 1987. 2605

Pattyn, F., Schoof, C., Perichon, L., Hindmarsh, R. C. A., Bueler, E., de Fleurian, B., Durand, G., Gagliardini, O., Gladstone, R., Goldberg, D., Gudmundsson, G. H., Huybrechts, P., Lee, V., Nick, F. M., Payne, A. J., Pollard, D., Rybak, O., Saito, F., and Vieli, A.: Results of the Marine Ice Sheet Model Intercomparison Project, MISMIP, *The Cryosphere*, 6, 573–588, doi:10.5194/tc-6-573-2012, 2012. 2599, 2600, 2605, 2606

Ross, N., Bingham, R. G., Corr, H. F. J., Ferraccioli, F., Jordan, T. A., Brocq, A. L., Rippin, D. M., Young, D., Blankenship, D. D., and Siegert, M. J.: Steep reverse bed slope at the grounding line of the Weddell Sea sector in West Antarctica, *Nat. Geosci.*, 5, 393–396, doi:10.1038/ngeo1468, 2012. 2609

Schoof, C.: Ice sheet grounding line dynamics: steady states, stability, and hysteresis, *J. Geophys. Res.*, 112, F03S28, doi:10.1029/2006JF000664, 2007a. 2599, 2600

Schoof, C.: Marine ice-sheet dynamics. Part 1. The case of rapid sliding, *J. Fluid Mech.*, 573, 27–55, doi:10.1017/S0022112006003570, 2007b. 2609

Thomas, R. H. and Bentley, C. R.: A model for Holocene retreat of the West Antarctic ice sheet, *Quaternary Res.*, 10, 150–170, doi:10.1016/0033-5894(78)90098-4, available at: <http://www.sciencedirect.com/science/article/pii/0033589478900984>, 1978. 2598

Vieli, A. and Payne, A. J.: Assessing the ability of numerical ice sheet models to simulate grounding line migration, *J. Geophys. Res.*, 110, F01003, doi:10.1029/2004JF000202, 2005. 2599

Weertman, J.: Stability of the junction of an ice sheet and ice shelf, *J. Glaciol.*, 13, 3–11, 1974. 2598, 2609

TCD

6, 2597–2619, 2012

Stable grounding lines on retrograde slopes

G. H. Gudmundsson
et al.

[Title Page](#)

[Abstract](#)

[Introduction](#)

[Conclusions](#)

[References](#)

[Tables](#)

[Figures](#)

◀

▶

◀

▶

[Back](#)

[Close](#)

[Full Screen / Esc](#)

[Printer-friendly Version](#)

[Interactive Discussion](#)



Table 1. Model parameters. The parameters B_0 , f_c and d are geometrical parameters that affect the shape of the bedrock (see Eq. 3). A and n are the rate factor and the stress exponent of Glen's flow law, respectively, C and m are the basal slipperiness and the stress exponent of Weertman's sliding law, and ρ and ρ_w are the specific densities of ice and ocean. The variable a is the surface mass balance in the units of ice equivalent. The number of days in a year is 365.25.

Parameter	Value	Units
B_0	300	m
f_c	5000	m
d_c	1000	m
A	10^{-24}	$\text{s}^{-1} \text{Pa}^{-3}$
n	3	
C	2.256×10^{-21}	$\text{ms}^{-1} \text{Pa}^{-3}$
m	3	
ρ	900	kg m^{-3}
ρ_w	1000	kg m^{-3}
a	0.3	ma^{-1}

Stable grounding lines on retrograde slopes

G. H. Gudmundsson
et al.

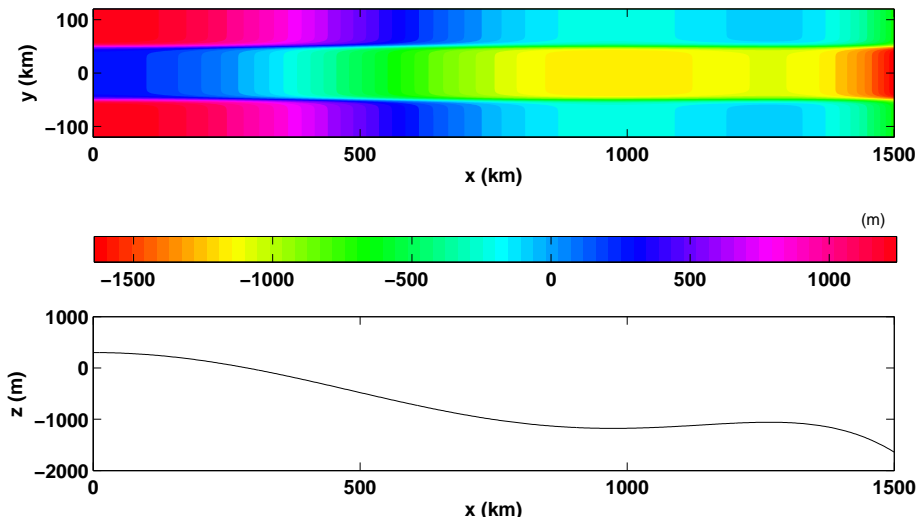


Fig. 1. Bedrock geometry. Upper panel: map-plane view of bedrock geometry with a corresponding colourbar below. Lower panel: longitudinal section of bed along the medial line ($y = 0$).

[Title Page](#)

[Abstract](#)

[Introduction](#)

[Conclusions](#)

[References](#)

[Tables](#)

[Figures](#)

◀

▶

◀

▶

[Back](#)

[Close](#)

[Full Screen / Esc](#)

[Printer-friendly Version](#)

[Interactive Discussion](#)

Stable grounding lines on retrograde slopes

G. H. Gudmundsson
et al.

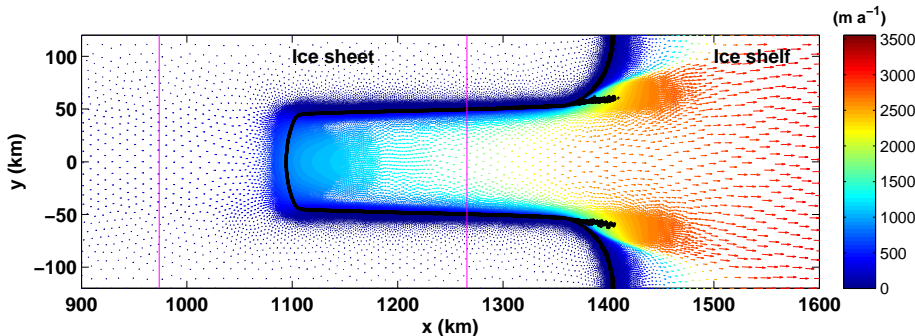


Fig. 2. Map-plane view of surface velocities obtained with the numerical code $\mathcal{U}a$ for a channel half-width of $w_c = 50$ km. Values of all other model parameters are listed Table 1. The two cyan lines at $x = 973.7$ km and $x = 1265.7$ km indicate where bedrock slope in x direction is equal to zero. The strip $973.7 \text{ km} < x < 1265.7 \text{ km}$ is an area of retrograde slope where the bed slopes upwards in x direction. The grounding line marking the division between grounded and floating ice is shown as a thick black line. The arrows represent surface velocities with the corresponding colourbar shown to the right.

[Title Page](#) | [Abstract](#) | [Introduction](#)
[Conclusions](#) | [References](#)
[Tables](#) | [Figures](#)

[◀](#) | [▶](#)
[◀](#) | [▶](#)
[Back](#) | [Close](#)
[Full Screen / Esc](#)

[Printer-friendly Version](#)

[Interactive Discussion](#)

Stable grounding lines on retrograde slopes

G. H. Gudmundsson
et al.

[Title Page](#)

[Abstract](#)

[Introduction](#)

[Conclusions](#)

[References](#)

[Tables](#)

[Figures](#)

◀

▶

◀

▶

[Back](#)

[Close](#)

[Full Screen / Esc](#)

[Printer-friendly Version](#)

[Interactive Discussion](#)

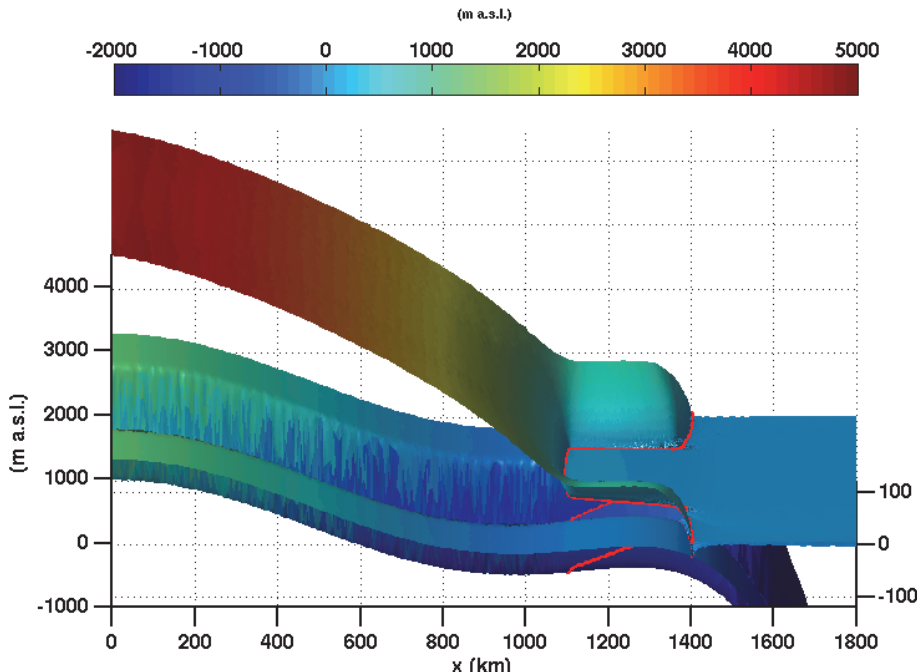


Fig. 3. A perspective plot of the steady-state geometry obtained with the numerical code $\mathcal{U}a$ for a channel half-width of $w_c = 50$ km. Shown is the upper and lower glacier surface and the ocean bathymetry. The grounding line is drawn as a red line along the upper and the lower glacier surface.

Stable grounding lines on retrograde slopes

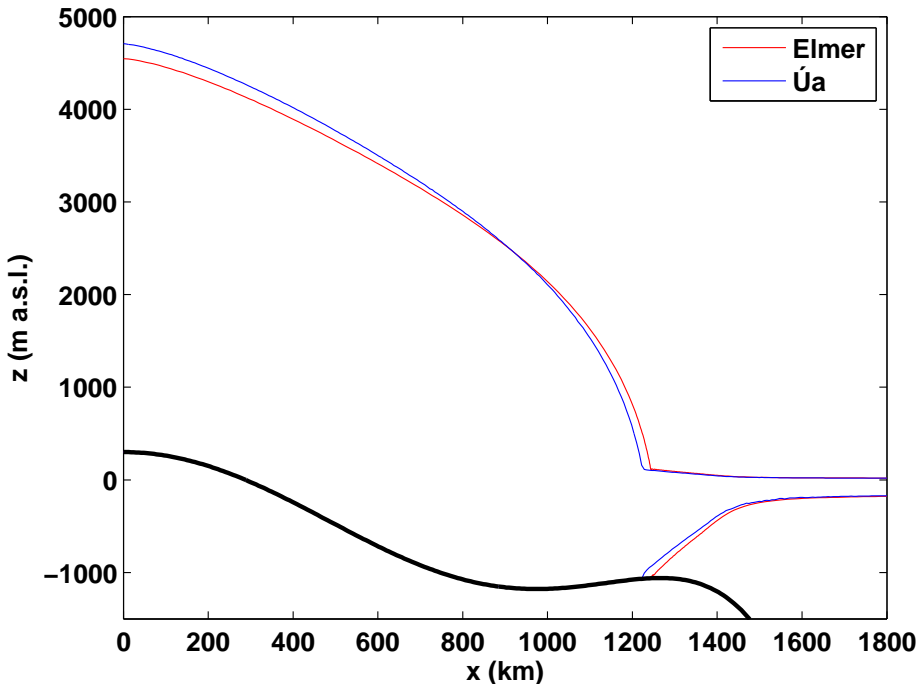
G. H. Gudmundsson
et al.

Fig. 4. Longitudinal surface profiles along the medial line ($y = 0$) obtained with both the full Stokes solver *Elmer/Ice* (red lines) and the vertically-integrated solver \bar{U}_a (blue lines). The calculations were done for a channel half-width of $w_c = 40$ km. The thick black line is the ocean floor.

[Title Page](#)
[Abstract](#) [Introduction](#)
[Conclusions](#) [References](#)
[Tables](#) [Figures](#)
[◀](#) [▶](#)
[◀](#) [▶](#)
[Back](#) [Close](#)
[Full Screen / Esc](#)

[Printer-friendly Version](#)
[Interactive Discussion](#)

